EFFECTS OF PROTEIN DOMAINS ON LOCALIZATION OF PENICILLIN-BINDING PROTEINS 2a AND 2b IN *BACILLUS SUBTILIS*

Yong Xue

Thesis submitted to the faculty of the
Virginia Polytechnic Institute and State University
in partial fulfillment of the requirement for the degree of
Master of Science
In
Biological Sciences

Committee members:
Chair: David L. Popham
Ann M. Stevens
Richard A. Walker
Zhaomin Yang

September 24, 2008
Blacksburg, VA

Keywords: *Bacillus subtilis*, penicillin-binding proteins (PBPs), localization, immunofluorescence

EFFECTS OF PROTEIN DOMAINS ON LOCALIZATION OF PENICILLIN-BINDING PROTEINS 2a AND 2b IN *BACILLUS SUBTILIS*

Yong Xue

ABSTRACT

Peptidoglycan not only protects bacterial cells against intracellular pressure but also provides the cells with a defined morphology. Penicillin-binding proteins (PBPs) catalyze the polymerization of the peptidoglycan in *Bacillus subtilis*. PBP2a and PBP2b are class B PBPs which have been known to have transpeptidase activities and they localize at different positions on the cell membrane. PBP2a spreads around the cylindrical wall as well as some at the septum, and PPB2b localizes exclusively to the septum and some at the cell poles. Both PBP2a and PBP2b are composed of four domains: S, N, P, and C domains from the N- to C- terminus. A FLAG epitope was tagged to the C-terminal ends of PBP2a and PBP2b. Cells with FLAG tagged PBP2a or PBP2b grow as well as wild type strain. Expression of PBP2a-FLAG and PBP2b-FLAG can be detected by western blotting using anti FLAG antibody. The expression of wild type PBP2a/PBP2b in these strains was tightly controlled by a xylose promoter. The FLAG fusion didn't influence the normal membrane localizations of PBP2a or PBP2b.

PBP2a/2b mutant strains with the S and/or N domains switched between PBP2a and PBP2b were constructed. All these domain-switch proteins were tagged with a FLAG at the C-terminus. The expression of these recombinant proteins can be detected by western blotting. None of these domain-switch proteins was able to complement the wild type PBP2a and PBP2b and cells with only these recombinant proteins but no wild type proteins were non-viable. Cellular localization of these domain switch proteins were visualized using immunofluorescence

microscopy. Proteins containing the PBP2a S domain had the same localization patterns as wild type PBP2a. Proteins that have the PBP2b S domain localized specifically at the septum and cell poles, which is similar to the wild type PBP2b. These results indicate that the S domain is the determinant to direct PBP2a and PBP2b to their cellular destinations.

ACKNOWLEDGEMENTS

Most of all, I would like to thank my thesis advisor, Dr. David L. Popham, a talented teacher and intelligent scientist. His critique and guidance has added substantial value to my research. I am so grateful for the time he carved out of his busy schedule to help me with every aspect of this research, for his careful guidance, and for his attentive teaching about research design and methods, scientific writing, and data analysis.

I would like to thank my committee membranes, Dr. Ann M. Stevens, Dr. Richard A. Walker and Dr. Zhaomin Yang for their advice and help during these years.

I would also like to thank all the people in Popham lab: Benjamin Orsburn, Emily Plass, Jared Heffron, Jessica McElligott, Pradeep Vasudevan, and past members Lin Liu and Michelle Dickens. Thanks for the fun and support.

Thanks to all the current and past students in the microbiology group. They made the labs like a family.

I cannot end without thanking my wife and my parents, on whose constant encouragement and love I have relied throughout my time at Virginia Tech.

TABLE OF CONTENTS

LIST OF FIGURES

LIST OF TABLES

REVIEW OF LITERATURE

Cell wall structure

The bacterial cell wall has functions of providing support for the maintenance of cell morphology, protecting the integrity of the cell membrane, and preventing cell breakage from the osmotic pressure. The cell wall is a huge net-like structure that surrounds the cell. The main structural component is peptidoglycan, which has a structure consisting of long glycan strands cross-linked by short peptides. In Gram-positive bacteria the cell wall is thick (15-80 nanometers), consisting of several layers of peptidoglycan (11). In Gram-negative bacteria, the cell wall is thin (10 nanometers) and composed of a single layer of peptidoglycan, with an outer membrane (18). There is a unique component in the outer membrane, lipopolysaccharide (LPS or endotoxin), which is toxic to animals. In Gram-negative bacteria the outer membrane is usually thought of as part of the cell wall.

The peptidoglycan backbone is made up of repeating disaccharide subunits N-acetylglucosamine (NAG) and N-acetylmuramic acid (NAM) connected by a beta 1, 4-glycosidic bond. Glycan strands are crosslinked by pentapeptides with the sequence L-Ala-D-Glu-L-meso-diaminopimelic acid-D-Ala-D-Ala in *Bacillus subtilis* and *E. coli*. D-Ala (4 position) from the side chain of a donor NAM links to diaminopimelic acid in the side chain of the acceptor NAM (18).

Peptidoglycan synthesis

Peptidoglycan biosynthesis is a two-stage process. In the first stage, the basic monomer unit is assembled. Enzymes catalyze this process in the cytoplasm or at the inner side of the cytoplasmic membrane (18). The initial precursor, UDP-NAG, is synthesized from fructose-6-P in four steps and is then used to generate UDP-NAM.

L-Ala, D-Glu, meso-diaminopimelic aid and D-Ala-D-Ala are successively added onto UDP-NAM by a series of enzymes and thus UDP-NAM-pentapeptide, the end product, is formed. The phospho-NAM-pentapeptide and NAG moieties are successively transferred onto the undecaprenyl phosphate carrier lipid by two membrane bound enzymes, the MraY translocase and MurG transferase, and thus the intermediate GlcNAc-MurNAc-(pentapeptide)- PP-undecaprenol, “lipid II”, is formed (61). Lipid II is then transferred to the outer side of the cytoplasmic membrane and the disaccharide units are polymerized.

In the second process, two enzymatic activities, transglycosylase and transpeptidase, play the most important roles, and they are found in a family of penicillin-binding proteins (PBPs) (21).The PBPs have been divided into three classes (Fig.1) according to their molecular weight (MW) and conserved amino acid motifs: the high MW (⩾60kD) Class A PBPs, the high MW Class B PBPs and the low molecular weight (⩽60kD) PBPs (18). The class A high-MW PBPs are bifunctional with transpeptidase activity in the C-terminal domain and a glycosyl transferase activity in the N-terminal domain. Glycosyl transferase activity carries out the polymerization of the glycan strands. The class B high-MW PBPs were once reported to possess a glycosyl transfer activity, even though their N-terminal domains do not show homology to those of the class A PBPs. However, glycosyl transfer activity of the class B PBPs has never been proven convincingly (14).

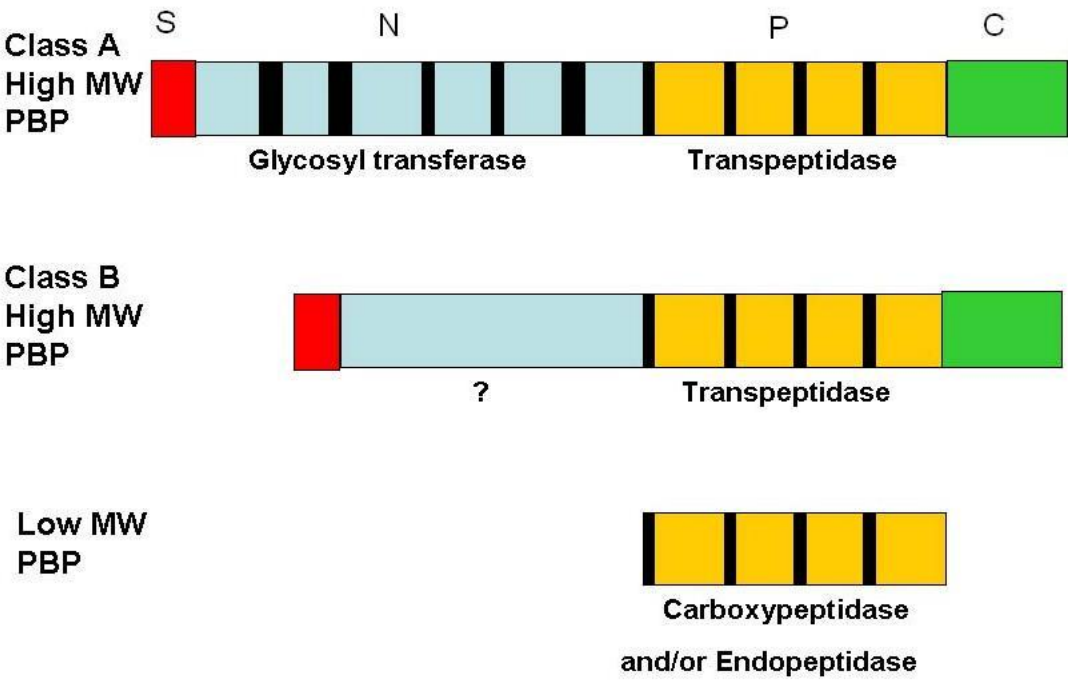

Figure 1. The domain structures of the class A and class B high MW PBPs and the low MW PBPs. Class A and B high MW PBPs are composed of S (signal, red block), N (blue), P (orange) and C (green) domains, with the N domain coding for glycosyl transferase and P domain functioning as transpeptidase. The function of the N-terminal domain of class B PBPs has not been demonstrated. Low MW PBPs have a single P domain with carboxypeptidase or endopeptidase activity. The conserved sequences (black blocks) in the P domain in all PBPs are integral to the active sites of each enzymatic activity as well as the target of penicillin.

Penicillin-binding proteins

Class A PBPs have bifunctional activities: glycosyl transferase in the N-terminal domain and transpeptidase in the C-terminal domain. In *Bacillus subtilis* there are four Class A PBPs: PBPs 1, 4, 2c, and 2d, encoded by *ponA*, *pbpD*, *pbpF*, and *pbpG* respectively. Deletion of *ponA* causes decreases in growth rate and sporulation efficiencies and the production of longer, thinner, and slightly bent cells (50). *pbpD* and *pbpF* genes show significant degrees of redundant function of *ponA*, the further loss of these genes from a *ponA* mutant exacerbates the phenotypic changes (49). *pbpF* and *pbpG* play a redundant role in sporulation. Deletion of both *pbpF* and *pbpG* leads to a severe sporulation defect (9).

As shown in Fig 1, there are 4 domains in class A PBPs, which we call the S, N, P, C domains. The S domain is a cytoplasmic domain containing several basic residues and an uncleaved signal peptide. The N- and P- domains contain the glycosyl transferase and transpeptidase active sites, respectively. The C-domain has no defined function and is highly variable (21).

Class B PBPs have only transpeptidase activity and are important for determining cell shape, making them different from class A PBPs (21). *B. subtilis* class B PBPs include PBP2a, PBP2b, PBP3, PBP4b (YrrR), PBPH (YkuA), and SpoVD, encoded by *pbpA, pbpB, pbpC, pbpI, pbpH,* and *spoVD*, respectively. PBP2a is involved in formation of the rod-shaped cell (44,64) and its sequence is very similar to that of a protein with the analogous function in *E. coli*, PBP2, which is required for the maintenance of the rod shape of the cell (57). Therefore, PBPH carries out the redundant function of PBP2a (64). PBP2b is essential for septation (68), and is most similar to the *E. coli* PBP3 (gene product of *ftsI*). SpoVD is required for the spore PG synthesis (9). PBP3 was found to be dispensable under the growth, sporulation, and germination conditions tested (44). PBP4b

is specifically expressed in the forespore, but its function is unknown (65).

In previous work (64), a *B. subtilis* strain with a *pbpH* single deletion was constructed, and there were no significant differences in phenotypes compared to the wild-type strain. Another strain, in which *pbpA* and *pbpH* were both deleted and a xylose-regulated *pbpH* gene was inserted into chromosome, had the appearance of a wild-type strain in the presence of xylose. When xylose was removed from the culture, cells of this double mutant swelled and then lysed. These results suggest that *pbpA* and *pbpH* play redundant roles in formation of the rod shaped peptidoglycan cell wall (64). Vegetative cells with a carboxy truncated form of PBP2b were viable but had a filamentous morphology (68).

There are six low-molecular-weight class PBPs in *B. subtilis*. PBP5 (encoded by *dacA*) and PBP5* (encoded by *dacB*) are D,D- carboxypeptidases, and DacC and DacF are predicted to have the same activity based on sequence similarity (18). The two remaining gene products (those encoded by *pbpE* (50) and *pbpX* (49)) are predicted to be D, D-endopeptidases according to their sequence similarity to the D, D-endopeptidase, PBP4, of *E. coli* (18).

Green fluorescent protein (GFP) fusions have been used to determine penicillin-binding protein localization during vegetative growth of *B. subtilis* (52,53). In these strains, *gfp* gene was associated with N-terminal of each PBP gene. In class A PBPs, PBP1 localized predominantly to the septum, PBP4 and PBP2c localized to both the septum and the lateral cell wall (53). In class B PBPs, PBP2b was found to localize exclusively to the septum. PBP2a, PBPH, and PBP4b (YrrR) appeared to be concentrated all around the membrane. PBP3 has a quite different localization pattern, it distributes in distinct spots around the cell periphery (53). Among the four low-MW PBPs involved in

vegetative growth, PbpX localized predominantly at the septum, PBP4a localized around the cell periphery and PBP5 had a disperse localization along the lateral wall (53).

In the Gram-positive bacterium *Streptococcus pneumoniae*, there are six PBPs. Three of them are bifunctional class A high MW PBPs- PBP1a, PBP2a, PBP1b; two of them are monofunctional class B high MW PBPs- PBP2x, PBP2b; the other one-PBP3, is a low MW carboxypeptidase (8). The crystal structure of PBP2x has been solved by X-ray crystallography (13,45). Research on PBPs in *S. pneumoniae* mainly focuses on high level β-lactam resistance properties in clinical strains. Only PBP2x, PBP2B, and PBP1a were reported to affect this characteristic, the other three PBPs did not. PBP2x displays septal localization and is involved in cell division. Much lab work has been done to select amino acid mutations in PBP2x that produce high level β-lactam resistance. These mutations include: His394Tyr, Leu403Phe, Arg512Tyr, Thr526Ser, Thr550Ala, Gln552Glu, Gly597Asp, Leu600Trp, and Gly601Glu (31,35). All these amino acid substitutions locate in or close to the conserved motifs (SXXK, SXN, KSG) of the transpeptidase domain.

In *E. coli*, there are 12 PBPs. Three are class A PBPs: PBP1a, PBP1b, PBP1c; two are class B PBPs: PBP2 and PBP3; the remaining seven are LMW PBPs. PBP1a and PBP1b are bifunctional PBPs, which have both transpeptidase and transglycosylase activities. PBP2 and PBP3 are monofunctional transpeptidases. PBP2 forms complexes with other proteins as a cell elongase and PBP3 is involved in formation of division septum. The function of PBP1c is unknown (51).

The PBPs are targets of the β-lactam family of antibiotics, including penicillin, cephalosporin, carbapenem, and monobactam. These antibiotics have the function of inhibiting PBP transpeptidase activities, which are involved in peptidoglycan

cross-linking in the final stage of bacteria cell wall synthesis, through irreversibly binding to the penicillin binding domains of PBPs (20). The active sites of the PBPs' penicillin-binding domains have three conserved motifs: SxxK, SxN (or YxN) and KTG (or HSG). Crystal structures of PBPs have been analyzed by X-ray diffraction and these three domains are found to locate close to each other (29). The serine residue of the SxxK motif is the key element for penicillin binding and peptide transfer reactions. The serine hydroxyl nucleophilic attack on the β–lactam carbonyl carbon of the penicillin hydrolyzes the β–lactam ring and transfers the penicilloyl moiety to serine, thus forming a serine ester-linked acyl enzyme. Enzyme deacylation is very slow or even completely inert, thus transpeptidase activity is inhibited. β–lactamases, another group of proteins which have the same conserved motifs with PBPs, have a rapid deacylation process and thus release biologically inactive penicillin (19).

The penicilloylation process has been used in PBP purification by affinity chromatography. 6-aminopenicillanic acid was bound to sepharose and PBPs covalently bound to it when detergent-solubilized membrane proteins flowed through the column. Hydroxylamine (NH_2OH) is the main reagent in the elution buffer. It cleaves the penicilloyl-enzyme bond and elutes PBPs out of column (6). Radiolabeled [^{14}C] penicillin G was used in 1972 to detect different PBPs (5). Membrane proteins were incubated with [^{14}C] penicillin G and then separated by polyacrylamide gel electrophoresis in the presence of sodium dodecyl sulfate (SDS). Five labeled components were separated in *B. subtilis*. These PBPs were named 1 to 5 according to their molecular masses.

Proteins involved in bacterial cell elongation and division

In *E. coli*, the maintenance of the cell's cylindrical shape during cell elongation and septation involves a set of network-specific proteins termed SEDS (shape, elongation, division, and sporulation proteins). The first morphogenetic network includes RodA

(encoded by *rodA*) (42,59) and class B high MW PBP2 (encoded by *pbpA*)(57), which are involved in maintenance of the rod shape of cells during cell elongation. Mutations in *rodA* or *pbpA*, or the inactivation of PBP2, block elongation and cause the production of spherical cells(22,56). These two genes are in one operon (42), and their gene products are expected to interact with each other (41). MreB, MreC, and MreD also belong to this network (62). MreB is a protein homologous to actin and polymerizes as a helix at the inner face of the membrane in *E. coli* and *B. subtilis* (25,54). This protein is required for rod shape maintenance and proper chromosome segregation (34). MreC was found to interact with MreB, MreD and itself(33,60). Localization studies found that MreB helix can be formed in cells without PBP2, but not in RodA, MreC, or MreD depletion strains (26,32). These findings led to the model that MreB forms a distinct helix as a bacterial cytoskeleton underneath the cell membrane and contacts the membrane through MreCD. MreCD interacts with PBP2 and ensures the insertion of new PG precursors to the cell wall.

Many of the division proteins in *B. subtilis* have homologues in *E. coli*, including FtsZ and FtsA, FtsW, DivIB (a homologue of FtsQ), FtsL, PBP2b (a homologue of FtsI) and YlaO (a homologue of FtsW). However, *B. subtilis* has no ZipA or FtsN homologue and contains another division protein, DivIC, which has no sequence homologue in *E. coli* (38). It appears that these proteins (DivIB, DivIC, FtsL and PBP2b) are recruited to the division site in a cooperative manner (17). This implies that there are distinct differences in the septation process between *B. subtilis* and *E. coli*.

Seven proteins described above are known to be required for septum formation in *B. subtilis*. The first one is FtsZ, which is conserved and abundant in all bacteria (about 5000 copies in an *E. coli* cell) (48). It is a tubulin homologue and forms a ring-like filamentous structure at the division site, termed the Z-ring. The Z-ring assembles at an

early stage of the cell cycle and is required to recruit other division proteins (16). In vegetative cells, FtsZ directly interacts with FtsA, which is homologous to actin. FtsA was shown to be a dimer and has weak ATPase activity. An FtsA null mutant is viable but extremely filamentous (3). The C-terminus of FtsZ is the interaction site for FtsA (63).

The next protein to assemble to the Z-ring is FtsW (encoded by *ftsW*)(7,30). By analogy with RodA and PBP2, it has been suggested that FtsW may act in concert with class B high MW PBP3 (encoded by *pbpB*) in *E. coli* cell division (24). The genes encoding FtsW and PBP3 are cotranscribed and their inactivation blocks cell division without affecting cell elongation. In another paper (43), *ftsW* expression was under control of an arabinose inducible promoter and *gfp* was fused to each division gene. When glucose was added instead of arabinose, depletion of FtsW had only minimal effect on localization of FtsZ, FtsA, ZipA, FtsQ and FtsL whereas GFP-FtsI (PBP3) failed to localize. These findings suggest that FtsW interacts directly with PBP3 and recruits it to the septum. As described above, depletion of FtsW has no effect on assembly of FtsZ, FtsA and other early proteins but blocks PBP2b localization, suggesting its intermediate position in the cell division pathway.

After assembly of FtsW, four other proteins, FtsL, DivIB, DivIC, and PBP2b (BDPs: the bitopic division proteins) localize to the division septum with unknown order. DivIB is homologous to FtsQ of *E. coli* and is required for division only at high temperature (2). The possible role of DivIB is to stabilize FtsL protein. FtsL is an unstable protein and can be easily degraded when DivIB is absent (10). DivIC has similar secondary structure to FtsL and interacts with FtsL by its C-terminal domain. The stability of DivIC is affected by both FtsL and DivIB (28,55). PBP2b is much more stable than FtsL. PBP2b has at least two functions: recruiting other BDPs to FtsZ ring and synthesizing PG with

transpeptidase activity.

Two factors are necessary for the regulation of timing and positioning of the cell division septum in *B. subtilis* and *E. coli*. First is a phenomenon termed "nucleoid occlusion". In cells where the nucleoid is replicating, FtsZ ring formation and cell division are inhibited. Recent work has found that it is DNA concentration, but not the presence of DNA that blocks cell division, which is supported by the observation that an FtsZ ring can form before DNA segregation completes in both *B. subtilis* and *E. coli* (12,67)

The other factor for division site selection is the Min system. Three genes are involved in this system: *divlVA, minC, minD*. MinC and MinD form a MinCD complex and act as a negative regulator for division at cell poles. DivIVA first targets to division sites and is stably associated with the cell poles after cell division (40). MinCD complex is also recruited to division sites by a direct interaction with DivIVA. DivIVA-MinCD remains associated with the pole site after division and thus prevent further division at this area. During cell division, minicell (polar divisions) formation is prevented, but the mechanism of MinCD inhibition of division is unclear (36).

Phenotypic effects of PBP mutants.

ftsI mutations have been made in *E. coli* to identify sequences that effect membrane localization and recruitment of other division proteins. David S. Weiss and coworkers generated *ftsI* mutants that had point mutations randomly by *Taq* DNA polymerase PCR amplification (66). PBP3 mutants that were unstable, defective in cytoplasmic membrane insertion, and transpeptidase activity were ruled out. Mutants that only had defects in division ring localization are found to have point mutations altering R23, L39, and Q46 amino acids. These residues are in the transmembrane helix and thus this region is

verified to be involved in PBP3 localization. These localization defects caused cells to become filamentous. Other PBP3 mutants defective in recruitment of FtsN to the division ring, which also resulted in longer cell shape, have point mutations altering G57, S61, L62 and R210, which are in the noncatalytic domain. These residues are close to each other in 3 dimensional structure of PBPs and might be an interaction site between PBP3 and FtsN (66).

Different truncations of *E. coli* PBP3 have been examined and results show that the first 56 amino acids of PBP3 are sufficient to target protein to the division site. Mutations at the putative interactive sites of the noncatalytic domain of PBP3 result in perturbation of cell division but don't disturb division site localization (47). A bacterial two-hybrid system was used to identify the PBP3 interaction network. Several truncated variants were tested for interactions with FtsL, FtsQ, FtsW. Data indicate that the first 70 residues are sufficient to bind FtsQ, the transmembrane region (aa 1-70) contains the FtsW binding site, and the membrane bound (1-250) region appears to interact with FtsL (27).

We are interested in identifying domain functions of *B. subtilis* PBP2a and PBP2b. The work presented here is to construct a series of strains that express *pbpA* or *pbpB* in which the S and/or N domains are switched between them. We study the phenotypic effects and localization of these mutants, and this will help us understand how these PBPs work together to maintain the normal cell shape.

MATERIALS AND METHODS

Bacterial strains and growth conditions

B. subtilis strains and plasmids used in this study are listed in Table 1 and Table 2. All *B. subtilis* strains were derived from PS832 and all *E. coli* strains were derived from JM109. Transformations of plasmid or chromosomal DNA into *B. subtilis* were done as described previously (1). *E. coli* strains were incubated in 2xYT medium (49) containing ampicillin (50 μg/ml). *B. subtilis* vegetative growth was at 37°C in 2xSG medium (37) containing appropriate antibiotics: chloramphenicol (3 μg/ml), spectinomycin (100 μg/ml), kanamycin (10 μg/ml), tetracycline (10 μg/ml), erythromycin (0.5 μg/ml) plus lincomycin (12.5 μg/ml). *B. subtilis* transformants were selected on 2xSG agar plates with appropriate antibiotics, 1% starch was added to plates to detect amylase activity. For xylose inducible promoter expression, 0.4% xylose was added to the medium.

Plasmid and strain construction

For *pbpA*S-*pbpB*NPC mutant construction, primers pbpAupPacI and pbpASBN were used to amplify the 140 bp *pbpA* S domain region from pDPV263 with the 21bp *pbpB* N domain sequence at the 3' end of the *pbpA* gene. This PCR product (ASBN) and primer pbpB2FLAGBamHI were then used to PCR amplify a 2.2kb fragment containing the *pbpA* S domain and the *pbpB* NPC domains from *pbpB* gene in pDPV274. A FLAG tag was added to the 3' end, and *PacI* and *BamHI* sites were added to the 5' and 3' end, respectively. The *pbpA*S-*pbpB*NPC fragment was then cloned into the pSWEET-bgaB vector (4) between the *PacI* and *BamHI* sites, generating plasmid pDPV357. pDPV357 was transformed into *E. coli* DPVE3 (JM109) and sequenced using primers pbpAupPacI, pbpBseq500rev, PbpBseq1320, pDPV274Rev, pbpB2FLAGBamHI to confirm that the PCR product had the correct sequence and no mutation. Different primers were used to construct pDPV359 (*pbpA*SN-*pbpB*PC), pDPV358 (*pbpB*S-*pbpA*NPC), and pDPV355 (*pbpB*SN-*pbpA*PC) using the same strategy.

Table 1. *B. subtilis* strains

Strain	Genotype	Transformation		Source or reference
		Donor	Recipient	
DPVB3	*cwlDorf1::Sp*	pDPV5	PS832	Laboratory stock
DPVB133	*ΔpbpH::Sp*	pDPV113	PS832	(64)
DPVB203	*pbpA::Cm:erm*	pCm::Erm	PS2465	(64)
DPVB360	*pbpA-FLAG, xylP-pbpA, ΔpbpH::Sp*	pDPV263	DPVB133	This work
DPVB391	*pbpB-FLAG, xylP-pbpB*	PDPV274	PS832	This work
DPVB561	*amyE*::pDPV355	pDPV355	PS832	This work
DPVB562	*amyE*::pDPV355, *pbpA*::Cm::Er	pDPV355	DPVB203	This work
DPVB563	*amyE::pDPV357*	pDPV357	PS832	This work
DPVB564	*amyE::pDPV358*	pDPV358	PS832	This work
DPVB565	*amyE::pDPV358, pbpA::Cm::Er*	pDPV358	DPVB203	This work
DPVB566	*amyE::pDPV359*	pDPV359	PS832	This work
DPVB567	*amyE::pDPV357, pbpA::Cm::Er*	pDPV357	DPVB203	This work
DPVB568	*amyE::pDPV359, pbpA::Cm::Er*	pDPV359	DPVB203	This work
DPVB569	*amyE::pDPV360*	pDPV360	PS832	This work
DPVB570	*amyE::pDPV360, pbpA::Cm::Er*	pDPV360	DPVB203	This work
DPVB571	*amyE::pDPV361*	pDPV361	PS832	This work
DPVB572	*amyE::pDPV361, pbpA::Cm::Er*	pDPV361	DPVB203	This work
PS832	wild type			Laboratory stock
PS2465	*pbpA::Cm*	pTMA4	PS832	(44)

Table 2. Plasmids

Plasmid	Construction or Description	Source or reference
pCm::Erm	Cm::Erm, antibiotic resistance switch from Cm to Erm	(58)
pDPV263	*pbpA*-FLAG is in opposite orientation to cat in pSG 1164	This work
PDPV274	*pbpB*-FLAG is in opposite orientation to cat in pSG 1164	This work
pDPV355	pSWEET vector with domain switch mutant gene: SN domain of *pbpA* was replaced by SN domain of *pbpB*.	This work
pDPV357	pSWEET vector with domain switch mutant gene: S domain of *pbpB* was replaced by S domain of *pbpA*.	This work
pDPV358	pSWEET vector with domain switch mutant gene: S domain of *pbpA* was replaced by S domain of *pbpB*.	This work
pDPV359	pSWEET vector with domain switch mutant gene: SN domain of *pbpB* was replaced by SN domain of *pbpA*.	This work
pDPV360	pSWEET vector with domain switch mutant gene: N domain of *pbpA* was replaced by N domain of *pbpB*.	This work
pDPV361	pSWEET vector with domain switch mutant gene: N domain of *pbpB* was replaced by N domain of *pbpA*.	This work
pDPV362	278bp *pbpB* region between SacII and SmaI was inserted into pMUTIN4	This work
pSWEET-bgaB	xylP-*bgaB*	(4)

Table 3. Primers for amplifying and sequencing of *pbpA/pbpB*

Primer name	Sequence	Restriction site added
pbpAupPacI	5'CGCTTAATTAATAGAAAAGGTGATGTTATGAGG	*PacI*
pbpASBN	5'CGCTTTTGTCGCAAGCACTTCCACAATAATCCAGG	
pbpANBP	5'CCAAAAAGGTTTGAATTTTCTGGTCAATTGTTAGTACAAC	
pbpA2FLAGBamHI	5'CGCGGATCCTTACTTGTCATCGTCGTCCTTGTAGTCGTTATCAGAAGACGTTGTGTTTTC	*BamHI*
pbpBupPacI	5'CGCTTAATTAAGTGAAAAACATACAGGAATGATTC	*PacI*
pbpSAN	5'GATCTGCTTGATGCCCAGTTCGCCGTTCGCTTTTCC	
pbpBNAP	5'CTGATTTTTGCAAATCAATATCAATGGTTAAATATAC	
pbpB2FLAGBamHI	5'CGCGGATCCTTACTTGTCATCGTCGTCCTTGTAGTCATCAGGATTTTTAAACTTAACC	*BamHI*
BSpbpA1	5'CGGATATCCCTTTAAAATGAAAACTGGC	
pbpAFLAGUP	5'GAATTCAATAGAAAAGGTGATGTTATGAGG	*EcoRI*
pbpAupXbaI	5'GCTCTAGAGGAGAAATAAACCAAAAAAGC	*XbaI*
pbpAtruncRev	5'ACTAGTGCGCTGTTCTTGCGTGGTCG	*SpeI*
pbpAseq440	5'CATTAGCTCTAAAGAAAGAC	
pbpAseq500rev	5'TCCGTTTTAGCTGAAGCTGG	
PbpAseq880	5'GGGCCAAAAAGCAAAAGTCG	
pDPV263Rev	5'ATCGCTCCAGTTTGAAGACC	
PbpAseq1320	5'AAATCTTGGCAAAACTTAGG	
pbpA3	5'TTCTTGCTTGATTTCGCC	
pbpA1FLAG	5'AATAAAGTCGATATGAAGAGTAGC	

pbpA2FLAG	5’TTACTTGTCATCGTCGTCCTTGTAGTCGTTATCAGAAGACGTTGTGTTTTC	
pbpA4	5’GCCATCAGAAGCATAAGC	
pbpB-Upstream	5’TTGCGAAAAAGAACGGCTTG	
pbpBFLAGUP	5’GTCGACGTGAAAAACATACAGGAATGATTC	*SalI*
PbpBseq440	5’GGCCGGGATATTACGTATTC	
pbpBseq500rev	5’TTTTGTATCCCGTAAAAATG	
PbpBseq880	5’GCCCAAGCTTTGATCCGAAC	
PbpBseq1320	5’CAGCAGATTCAGGCCGCAAC	
pDPV274Rev	5’ATATCCCGCACCTTTTTCG	
pbpB3	5’CTAAAAGCAGGACAAAGC	
pbpB1FLAG	5’CAATGAAAAATAGCCTGCACTACC	
pbpB2FLAG	5’TTACTTGTCATCGTCGTCCTTGTAGTCATCAGGATTTTTAAACTTAACC	
pbpB4	5’CAAGAGACCGTTCACTCC	

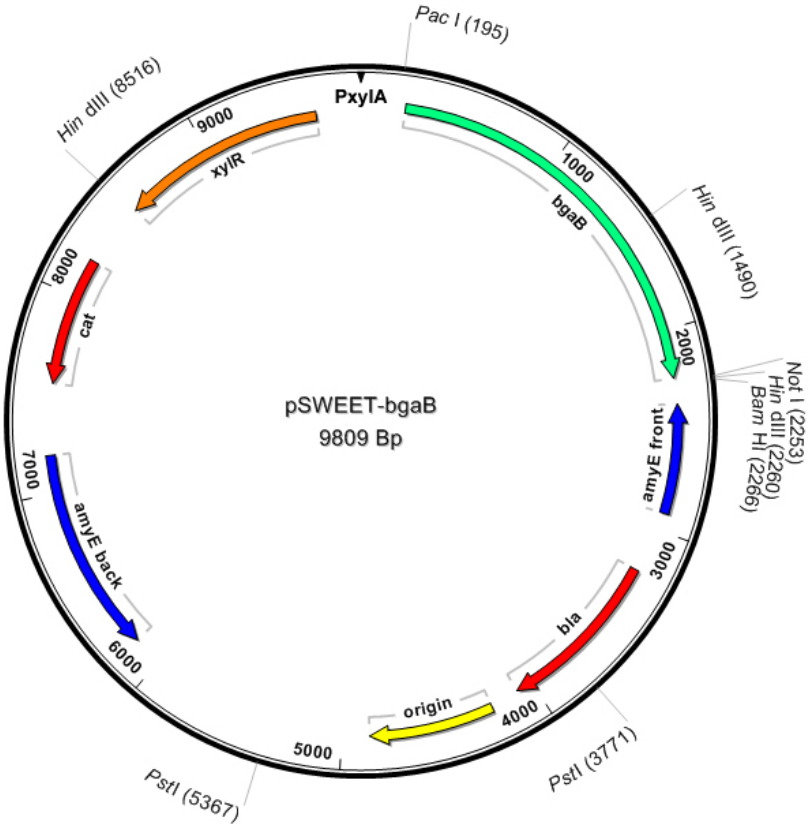

Figure 2. Map of plasmid pSWEET-bgaB. Plasmid pSWEET-bgaB (4) replaces the *amyE* locus in the *B. subtilis* chromosome via double crossover recombination and provides chloramphenicol resistance (cat). The plasmid also has an *E. coli* replication origin and ampicillin resistance cassette (bla). The xylose regulated promoter (P_{xylA}) allows control of an inserted gene's expression by adding xylose to the medium. Six PBP domain switch alleles were cloned into pSWEET-bgaB between *PacI* and *BamHI* and then integrated into the *B. subtilis* chromosome.

To get *pbpA*S-*pbpB*N-*pbpA*PC, the *pbpB*SN-*pbpA*PC PCR product was used as template. ASBN PCR product and primer pbpA2FLAGBamHI were used as forward and reverse primers to amplify a 2kb fragment. The fragment was cloned into pSWEET-bgaB through *PacI* and *BamHI* sites, generating pDPV360. The insert into the plasmid was sequenced and confirmed to be correct. By using the same method, pDPV355 (*pbpB*S-*pbpA*N-*pbpB*PC) was obtained.

These plasmids were linearized by a restriction enzyme cut at an *XhoI* site in the pSWEET-bgaB vector. Linearized plasmids were transformed into the *B. subtilis* wild type strain, PS832, and the *pbpA* depletion strain, DPVB203. Transformants were selected on 2xSG plates containing chloramphenicol (PS832 transformants) or chloramphenicol and erythromycin plus lincomycin (DPVB203 transformants) to allow the plasmids to integrate into the chromosome at the *amyE* locus via double crossover. Transformants were verified by a starch hydrolysis assay.

From pDPV355, a 278 bp region internal to *pbpB* was cut out using *SacII* and *SmaI* and ligated into the pMUTIN4 vector, generating pDPV362. The plasmid was verified by sequencing and then transformed into DPVE2 (JM107, Rec+) to produce plasmid concatemers. pDPV362 concatemers were transformed each domain switch *B. subtilis* strain with selection for MLS^R transformants on 2XSG plates containing 0.4% xylose.

SDS-PAGE and western blotting analysis

Cells from 100 ml exponential-phase cultures (optical density at 600 nm [OD_{600}] of ~1.0) grown in 2xSG medium were harvested by centrifugation (8,000 g, 10 min), washed with 25 ml of cold PBS buffer (137 mM NaCl, 2.7 mM KCl, 4.3 mM Na_2HPO_4, 1.4 mM KH_2PO_4, pH 7.3) with 1 mM beta-mercaptoethanol and Protease Inhibitor Cocktail Tablets (Roche), centrifuged (8,000 g, 10 min), resuspended in 2.5 ml of PBS

buffer, and kept cold on ice. Cells were broken by sonication, the lysate was cleared by centrifugation (8,000 g for 10 min at 4°C). The supernatant was stored at -80°C and used for SDS-PAGE analysis.

For SDS-PAGE, 20 µl of crude supernatant protein were mixed with sodium dodecyl sulfate (SDS) sample buffer and boiled for 5 min, and proteins were separated by SDS–7.5% polyacrylamide gel electrophoresis (PAGE) at 200 v for 45 minutes. After electrophoresis the proteins were transferred to Hybond-P membrane in transfer buffer (3 g of Tris base/liter, 14.4 g of glycine/liter, 20% methanol [vol/vol]), and the membranes were subjected to immunoblotting as described in the manufacture's instructions of the BM Chromogenic Western Blotting Kit (Roche). Blots were probed with anti-FLAG M2 monoclonal antibody (2mg/ml) (Stratagene) and alkaline phosphatase labeled anti-mouse IgG/anti-rabbit IgG (Roche). Alkaline phosphatase substrate solution (NBT/X-phosphate solution) (Roche) was used for chromogenic detection.

PBP detection

B. subtilis cells were incubated in 2xYT medium at 37°C until the OD600 reached 0.5. Cells were harvested by centrifugation and resuspended in 1 ml of cold 50 mM Tris-HCl (pH 7.5), 1 mM $MgCl_2$, 1 M KCl, 0.1 mM PMSF, and centrifuged again. The cell pellets were resuspended in 1 ml of buffer A (100 mM Tris-HCl (pH 8.0), 1 mM $MgCl_2$, 1 mM β-mercaptoethanol, 0.1 mM PMSF). The cells were broken by sonication and the cell suspensions were centrifuged at 13,000 g for 10 min to remove large debris. Supernatant was centrifuged at 48,000 g for 1 hour at 4°C and the pellet was resuspended in 50 µl of buffer B (50 mM Tris-HCl (pH 8.0), 1 mM β-mercaptoethanol, 0.1 mM PMSF). The protein concentrations of membrane samples were determined by Lowry assay (39). PBPs were detected using Bocillin (FL penicillin, Invitrogen). 50 µg of membrane proteins was incubated with 25 mM Bocillin in a total volume of 20 ml for 30

min at 37 °C. Proteins were separated by 7.5% SDS-PAGE. PBPs were detected using a Typhoon imager scanner (GE Healthcare) with excitation at 532 nm and emission at 526 nm.

Cell preparation for immunofluorescence microscopy

Cell fixation, permeabilization, and staining were carried out as previously described (46). *B. subtilis* cultures were grown in 2xYT at 37 °C until an OD600 ~0.5. 0.5 ml of culture were harvested and pelleted by centrifugation at 4000 g for 1 min and resuspended in 1.5 ml fixation buffer containing 4.4% (wt/vol) paraformaldehyde and 28 mM $NaPO_4$ pH7.2 at 37 °C for 30 min. Cells were then washed three times with PBS and resuspended in 100 µl GTE buffer (50 mM glucose, 20 mM Tris-HCl pH 7.5, 10 mM EDTA) and digested with 0.2 mg/ml lysozyme at room temperature for 5 min. After washing twice with PBS buffer, cells were resuspended in 100 µl PBS, and applied to poly-lysine coated slides at room temperature for 30 min. Then slides were washed with PBS twice, blocked with 4% (wt/vol) BSA in PBS and incubated for 30 min at room temperature. Slides were incubated with 0.625 µg/ml anti-FLAG antibody (Stratagene) in 0.2% BSA for 1 hour at room temperature. After washing 3 times with PBS, slides were incubated with 5 µg/ml diluted biotinylated goat anti-mouse IgG (Invitrogen) in 0.2% BSA for 1 hour at room temperature. After washing three times with PBS, slides were incubated with 0.5 µg/ml Cy3-streptavidin (Jackson ImmunoResearch Lab), and 1 µg/ml of DAPI dye for 1 hour at room temperature. Slides were then washed three times with PBS, and mounted with Gold anti-fade reagent (Invitrogen). Cells were visualized using Delta Vision Core and personalDV Microscopy System with an Olympus IX71 microscope. The exposure time is 800 ms for DAPI, and 500 ms for Cy3.

RESULTS

PBP2a and PBP2b domain interface determination.

The amino acid sequences of 63 PBPs from different species have been aligned and several conserved regions and sequences have been found among them (21). Figure 3 shows the conserved sequence motifs of several Class B HMW PBPs in *B. subtilis, S. pneumoniae* and *E. coli.* The dicarboxylic acids D (39) (the numbers after each amino acid initial in this paragraph indicate the positions of these amino acids in the protein) in PBP2a and E (45) in PBP2b are immediately downstream of the N-terminal hydrophobic core that functions as a signal sequence and membrane anchor. Thus M (1)→V (38) of PBP2a and M (1)→G (44) of PBP2b were defined to be the S domains. Based on the crystal structure of *S. pneumoniae* PBP2x(45), motif 4 has been found to be conjunction of β6 strand at the C-terminal end of the non-penicillin binding domain and α1 helix at the N-terminal end of the penicillin binding domain. Therefore, homologous motif 4 of *B. subtilis* PBP2a and PBP2b are assumed to be the intermodule junction. Thus D (39)→I (321) of PBP2a and E (45)→I (244) of PBP2b were defined as the N domains.

Construction and verification of domain switch mutants.

In order to identify the structural determinants for PBP cellular localizations, the S and/or N domains between PBP2a and PBP2b were switched. These mutant alleles were cloned into the pSWEET-bgaB vector with addition of a FLAG tag at their C-terminal ends. Alleles were integrated into the chromosomes of the wild type PS832 strain and a *pbpA* mutant strain (for complementation studies) through double crossover at the *amyE* site. The *amyE* site integration of pSWEET plasmids was verified by the starch utilization assay. *amyE* encodes for amylase which can hydrolyze starch added in the agar plate and the plate will become blue when treated with iodine. For strains in which *amyE* were deleted, a clear hydrolysis zone around the colony disappears,

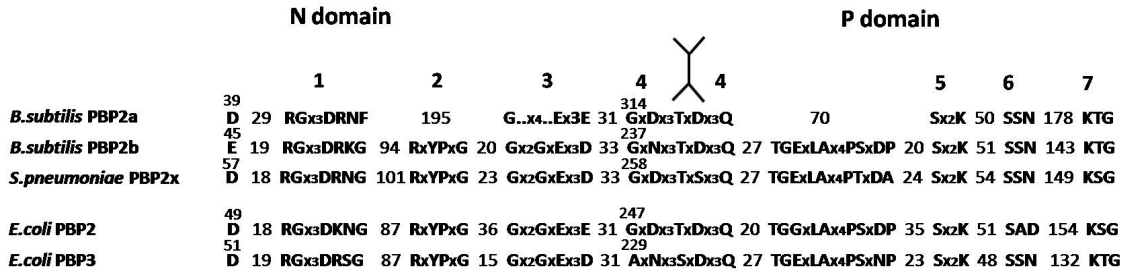

Figure 3. Several Class B PBPs conserved sequences in *B. subtilis*, *E. coli* and *S. pneumoniae*. The bold numbers above the alignments show the conserved domains for each PBP and the numbers between each alignment indicate the amino acid numbers of the gap. The numbers right above the amino acids indicate their position numbers and the intermodule junction separating the N and P domains is noted within motif 4 of each PBP. The first amino acid shown for each protein (D or E) was chosen as the end of the S domain. Figure adapted from (21).

indicating correct insertion of the pSWEET plasmids. For these strains, expression of the domain switch mutant genes was regulated by adding or removing xylose.

As shown in Figure 4, six domain switch mutants were constructed. DPVB564 and DPVB563 contain PBP2a and PBP2b coding genes, respectively, in which the S domain coding sequences were exchanged between them. For DPVB569 and DPVB571, the N domain coding sequences of PBP2a and PBP2b were switched. In DPVB561 and DPVB566, both the S and N domains were switched.

Phenotypes of PBP2a-FLAG and PBP2b-FLAG control strains.

To study the normal localization of PBP2a and PBP2b and phenotypic effects of the C-terminal linked FLAG tag, two control strains were constructed. A full length *pbpA* gene with a C-terminal FLAG sequence was cloned into pSG1164. The resulting plasmid, pDPV263, was transformed into *pbpH* strain DPVB133 and integrated into the chromosome via single crossover at the *pbpA* region, generating a strain (DPVB360) with *pbpA-FLAG* and xylose controlled *pbpA*. Another strain (DPVB391) was obtained by transforming the wild type PS832 strain with pDPV274 (pSG1164 with *pbpB-FLAG)*. This strain contains *pbpB-FLAG* and xylose controlled *pbpB*.

The growth rates of DPVB360 and DPVB391 were measured. Cells were inoculated in 2xSG medium with (0.4%) or without xylose at 37°C and OD600 values were recorded until it reached 1.5. From Figure 5, it appears that adding or removal of xylose doesn't affect cell growth. They all have a similar doubling time, 21 minutes, which is the same as wild type PS832. In the absence of xylose, cells only express PBP2a/2b-FLAG, and there's no wild type PBP2a/2b. Phase contrast microscopy of cells grown at log-phase revealed that DPVB360 and DPVB391 cells are morphologically identical to wild type cells (data not shown).

The wild type PBP2a/2b in DPVB360 and DPVB391 were controlled by a xylose promoter. We used fluorescence labeled penicillin (Bocillin) to visualize the PBPs in

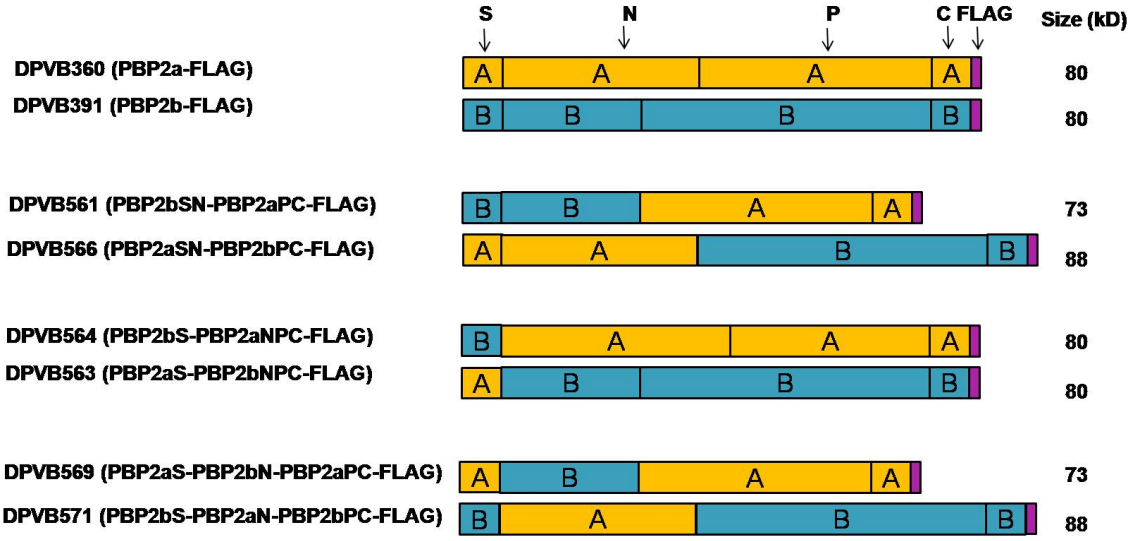

Figure 4. PBP2a and PBP2b structures and mutant construction. Pbp2a regions are depicted in orange and PBP2b in blue. Purple blocks represent the FLAG tag. Four domains are present in both PBP2a and PBP2b: S, N, P, and C. The calculated molecular weights of each protein are indicated on the right. The various molecule weights are due to the different sizes of the N and P domains of PBP2a and PBP2b.

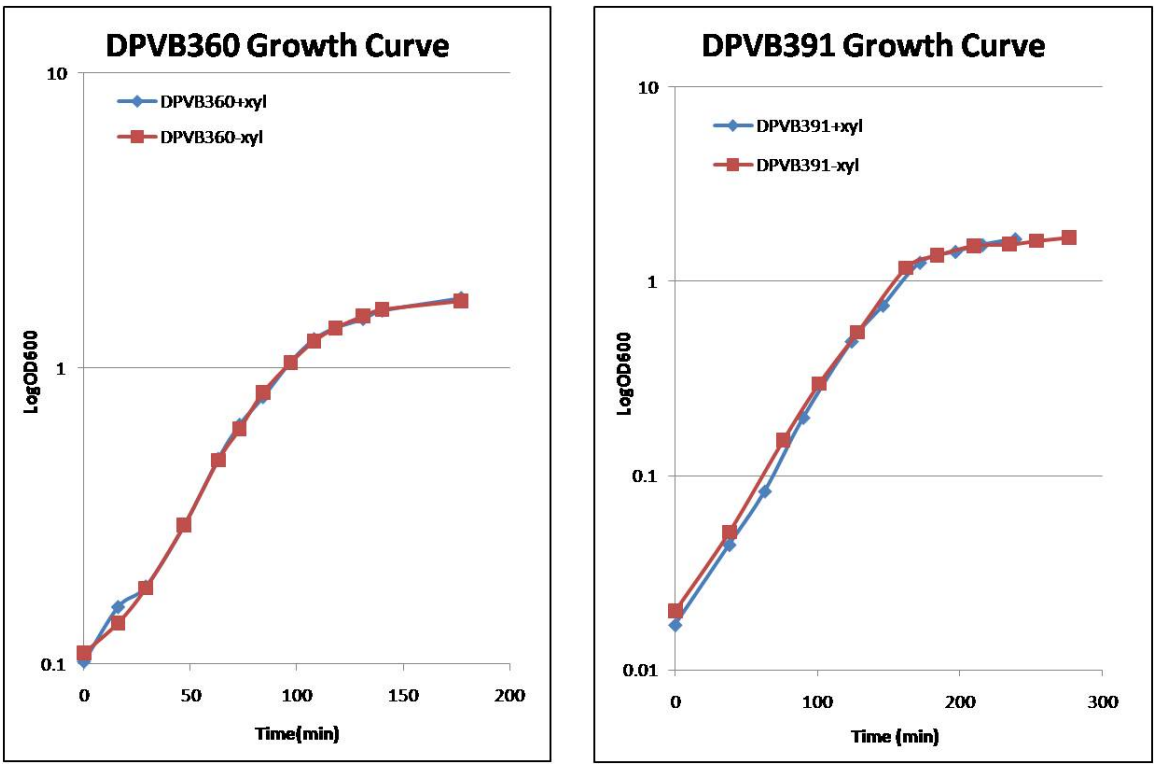

Figure 5 Growth of control strains. DPVB360 and DPVB391 strains were grown in 2xSG medium with or without 0.4% xylose at 37°C with aeration. OD600 was measured every 20 min until it reaches 1.5.

DPVB391 strains. Membranes were purified and separated by 7.5% SDS-PAGE from cultures with (0.4%) and without xylose. We observed that in the presence of xylose, both PBP2b and PBP2b-FLAG were expressed, while there was no wild type PBP2b in the absence of xylose (Figure 6). The result indicates that the xylose promoter can fully control the expression of downstream proteins.

Expression of FLAG tagged PBP2a/2b was further confirmed by western blotting. DPVB360 and DPVB391 grew in 2xSG without xylose until OD600~1.0. Cell extracts were saved and samples with 400 μg total protein were loaded onto a SDS-PAGE gel. Western blotting was done using anti-FLAG antibodies (Figure 7, lane 2 and 3). 80 kD PBP2a-FLAG and 79kD PBP2b-FLAG bands were detected in accordance with their calculated molecular weight.

Localization patterns of PBP2a and PBP2b were performed by detecting FLAG positions using anti-FLAG antibody, Biotinylated IgG, Cy3-streptavidin and DAPI (DNA stain) (Figure 8). Cells from a log-phase culture of the wild type strain PS832 were used as a negative control and gave no Cy3 signal. PBP2a-FLAG localized in the cylindrical wall as well as some septal locations. PBP2b-FLAG exclusively localized at the septum and some at the cell poles after cell division. These localization specificities are consistent with previous studies(53). These findings indicate that PBP2a-FLAG and PBP2b-FLAG are functionally equivalent to wild type PBP2a/2b in vivo.

The faint lanes with larger MW (85kD, 110kD, 170kD) on the immunoblot membrane (Figure 7) should come from the cross reactions of native proteins in the cell with antibodies, since membranes from wild type strain PS832, which doesn't have FLAG tag, have the same band patterns as others (Figure 7, lane 1). These cross reactions might interfere when we need to visualize the FLAG localization in vivo. Actually, we observed the background stains in the areas between the septum and cell pole when doing Cy3 staining of PBP2b control strains. To weaken the nonspecific background, we tried to treat cells with a series of diluted antibodies and dyes: 5 μg/ml, 2.5 μg/ml, 1.25 μg/ml,

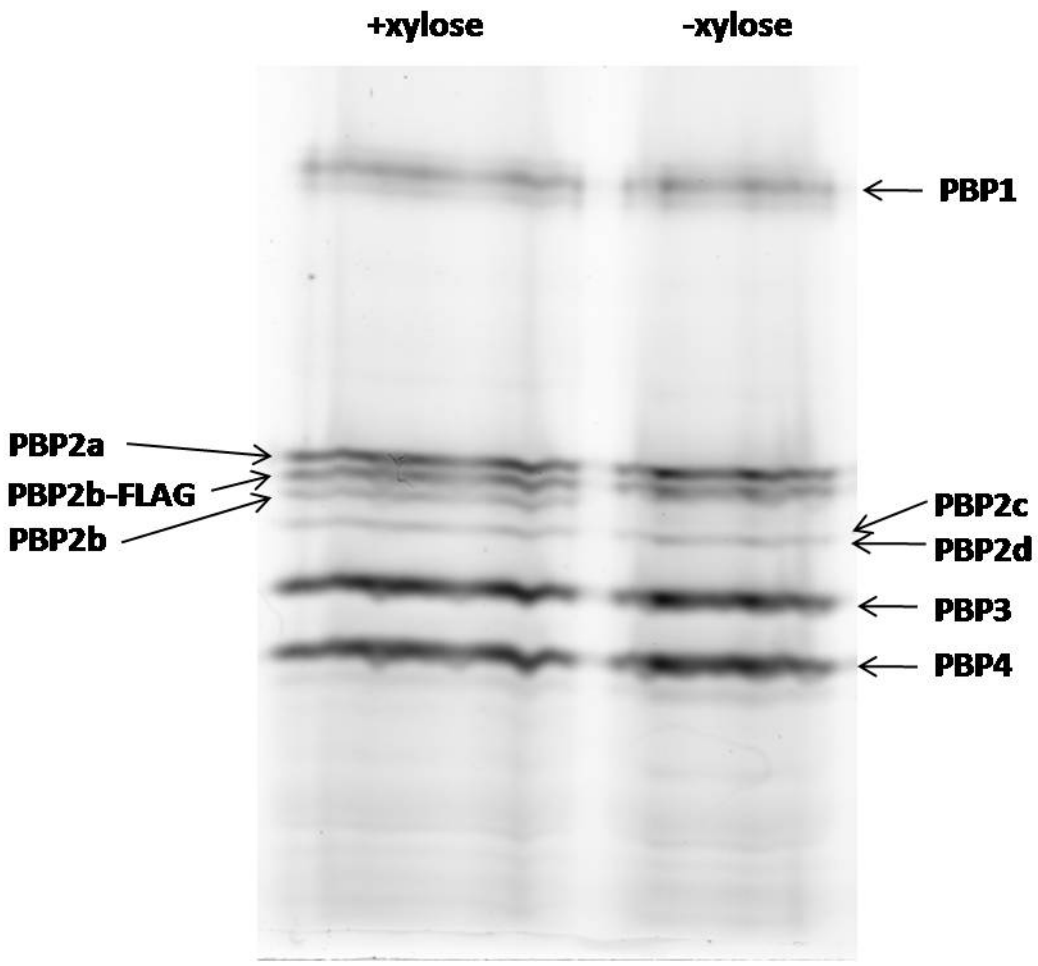

Figure 6. Expression of PBP2b in DPVB391 controlled by xylose promoter.
Membranes were purified from cultures with (left) and without (right) xylose at OD600 ~0.5. 25 μg proteins were incubated with Bocillin, separated on an SDS-7.5% PAGE gel, and were detected using a Typhoon imager scanner.

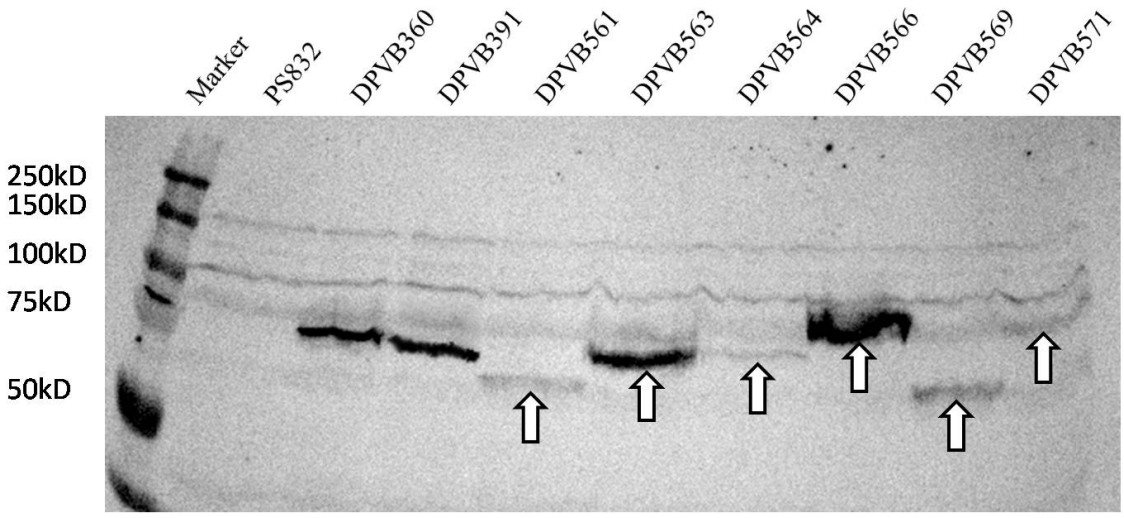

Figure 7. Western blotting analysis of PBP2a and PBP2b expressions in control and mutant strains. All strains were grown in 2xYT medium at 37°C until the OD600 reached 1.0. All mutant strains were incubated with 0.4% xylose (DPVB561, DPVB563, DPVB564, DPVB566, DPVB569, and DPVB571). Proteins from whole cell extracts were separated by 7.5% SDS-PAGE. Anti-FLAG antibody was used for detection of FLAG-tagged PBPs. Protein bands of the domain switch mutants are indicated by the arrows.

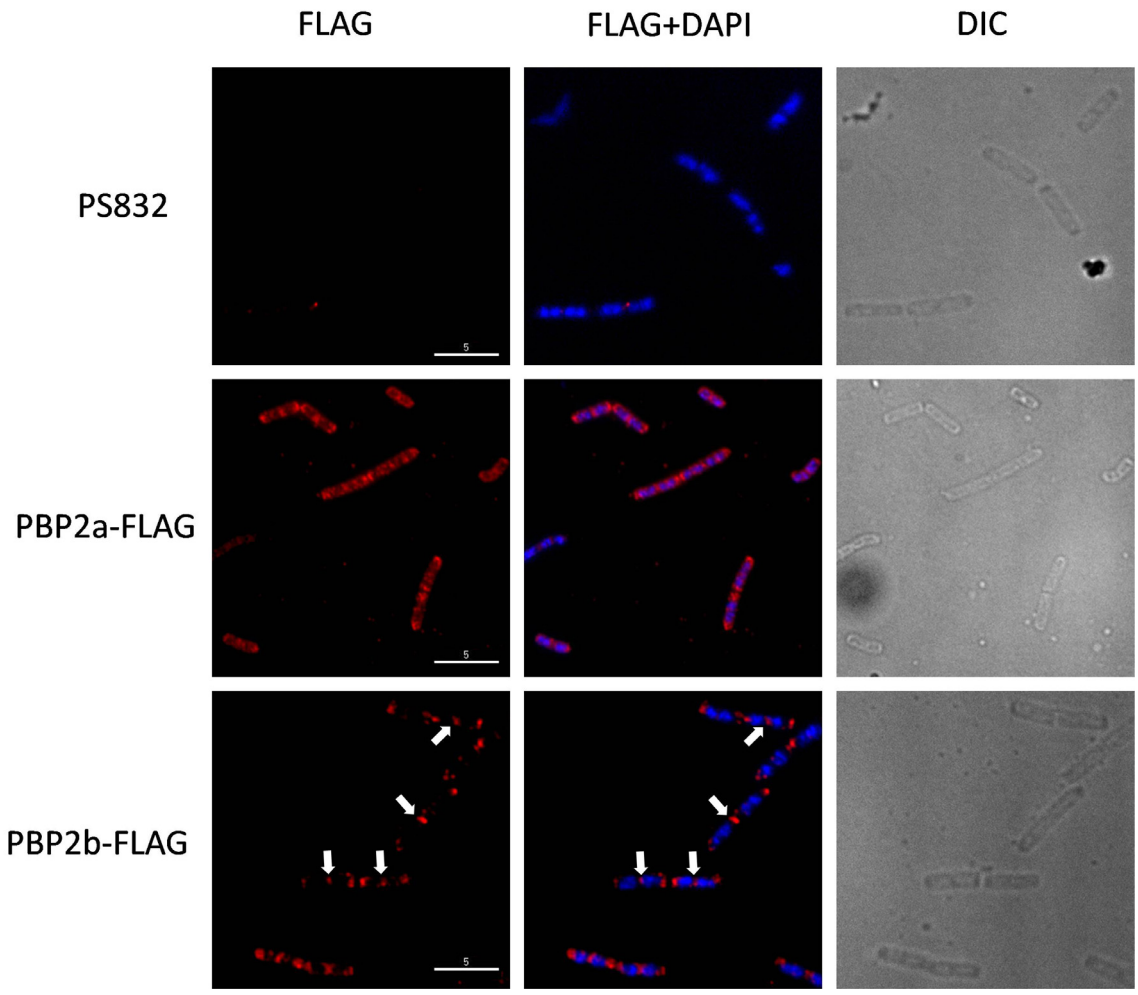

Figure 8. Localization of PBP2a and PBP2b. The figure shows a Cy3 staining of FLAG tagged PBPs (red), an overlay of DAPI staining of nucleoids (blue) and Cy3, and a differential interference contrast (DIC) image for comparison. Arrows point to PBP localizations at the midcell. The white bars represent 5 μm and all pictures are at the same magnification. Exposure time: 800 ms for DAPI and 500 ms for Cy3.

0.625 μg/ml, 0.312 μg/ml, 0.156 μg/ml for anti-FLAG antibody, 10 μg/ml, 5 μg/ml, 2.5 μg/ml, 1.25 μg/ml for biotinylated goat anti-mouse antibody, and 1 μg/ml, 0.5 μg/ml, 0.25 μg/ml for Cy3-streptavidin. Finally, we found the combination of 0.625 μg/ml of anti-FLAG antibody, 5 μg/ml of Cy3-streptavidin and 0.5 μg/ml Cy3-streptavidin gave the best band patterns (Figure 8). All 6 mutant cells were incubated using antibodies and dyes with the same concentrations.

Expression of PBP2a/PBP2b variants.

All six domain switch mutants were grown in the presence of xylose, allowing expression of FLAG tagged proteins. Membrane samples from log-phase cells grown at 37°C in 2xYT medium were prepared with the same total protein contents (~400 μg) and analyzed by SDS-PAGE then probed by anti-FLAG antibody (Figure 7). Result shows that all six strains can produce FLAG tagged proteins with expected molecular weights. PBP2aS-PBP2bNPC (lane 5) and PBP2aSN-PBP2bPC (lane 7) have similar expression levels as the positive controls (lane 2 and lane 3). The abundance of the other 4 recombinant PBPs (PBP2bS-PBP2aNPC, PBP2bSN-PBP2aPC, PBP2aS-PBP2bN-PBP2aPC, and PBP2bS-PBP2aN-PBP2bPC) are much lower.

Complementation studies of PBP2a/PBP2b variants.

We were interested in figuring out if the domain switched proteins still retained some of the wild type PBP functions. For *B.subtilis* transformation, 0.3 ml of competent cells at stationary phase (OD600 at 2.5~3.0) were transformed with 1 μl of 1μg/μl chromosomal DNA or 5 μl of 400 ng/μl plasmid DNA.

For a *pbpA* gene complementation study (Table 4), a *pbpA* deletion mutant strain, DPVB203, was used for transforming with the 6 domain switch constructs. These transformants were then transformed with chromosomal DNA of DPVB133 in which *pbpH* was deleted with insertion of a spectinomycin resistant cassette. It is known that

Table 4. *pbpA* and *pbpB* complementation experiments

Recipient cell	Genotype	Donor DNA	Reason	Colony Number /μg DNA
DPVB565	*amyE*::pSWEET-BS-ANPC *pbpA*::Cm::Er	VB133 chromosome	*pbpA* complementation	0
DPVB565	*amyE*::pSWEET-BS-ANPC *pbpA*::Cm::Er	VB3 chromosome	Competent cell control	~300
DPVB564	*amyE*::pSWEET-BS-ANPC	VB133 chromosome	Competent cell and DNA control	~200
DPVB564	*amyE*::pSWEET-BS-ANPC	pDPV 362	*pbpB* complementation	5
PS832	Wild type	VB133 chromosome	Competent cell control	~200
PS832	Wild type	pDPV 362	DNA control	0
DPVB562	*amyE*::pSWEET-BSN-APC *pbpA*::Cm::Er	VB133 chromosome	*pbpA* complementation	0
DPVB562	*amyE*::pSWEET-BSN-APC *pbpA*::Cm::Er	VB3 chromosome	Competent cell control	52
DPVB561	*amyE*::pSWEET-BSN-APC	VB133 chromosome	Competent cell control	~200
DPVB561	*amyE*::pSWEET-BSN-APC	pDPV 362	*pbpB* complementation	9
DPVB563	*amyE*::pSWEET-AS-BNPC	pDPV 362	*pbpB* complementation	4
DPVB563	*amyE*::pSWEET-AS-BNPC	VB133 chromosome	Competent cell control	~200
DPVB567	*amyE*::pSWEET-AS-BNPC *pbpA*::Cm::Er	VB3 chromosome	Competent cell control	~300
DPVB567	*amyE*::pSWEET-AS-BNPC *pbpA*::Cm::Er	VB133 chromosome	*pbpA* complementation	0

Table 4. Continued.

Recipient cell	Genotype	Donor DNA	Reason	Colony Number /μg DNA
DPVB566	*amyE*::pSWEET-ASN-BPC	pDPV 362	*pbpB* complementation	2
DPVB566	*amyE*::pSWEET-ASN-BPC	VB133 chromosome	Competent cell control	~300
DPVB568	*amyE*::pSWEET-ASN-BPC *pbpA*::Cm::Er	VB3 chromosome	Competent cell control	~300
DPVB568	*amyE*::pSWEET-ASN-BPC *pbpA*::Cm::Er	VB133 chromosome	*pbpA* complementation	0
DPVB570	*amyE*::pSWEET-AS-BN-APC *pbpA*::Cm::Er	VB133 chromosome	*pbpA* complementation	0
DPVB570	*amyE*::pSWEET-AS-BN-APC *pbpA*::Cm::Er	VB3 chromosome	Competent cell control	~200
DPVB569	*amyE*::pSWEET-AS-BN-APC	VB133 chromosome	Competent cell control	~200
DPVB569	*amyE*::pSWEET-AS-BN-APC	pDPV 362	*pbpB* complementation	3
DPVB572	*amyE*::pSWEET-BS-AN-BPC *pbpA*::Cm::Er	VB133	*pbpA* complementation	0
DPVB572	*amyE*::pSWEET-BS-AN-BPC *pbpA*::Cm::Er	VB3	Competent cell control	~200
DPVB571	*amyE*::pSWEET-BS-AN-BPC	VB133	Competent cell control	~200
DPVB571	*amyE*::pSWEET-BS-AN-BPC	pDPV 362	*pbpB* complementation	6

pbpH has redundant function with *pbpA*, and cells with the *pbpA* deletion are still viable (64). Transformants were selected for Sp^R on plates with xylose added, but no viable colonies were obtained. As controls, DPVB3 chromosomal DNA, with an unrelated Sp resistance marker, was transformed into these *pbpA* deletion strains and VB133 chromosome DNA was transformed into a strain with wild type *pbpA*. Both controls gave viable transformants. These results indicate that domain switch mutant PBPs can't complement wild type *pbpA* functions.

For a *pbpB* functional complementation assay (Table 4), strains contained the domain switch coding sequences at the *amyE* locus were transformed with a *pbpB* null allele. To eliminate the wild type *pbpB* gene, the pDPV362 plasmid with the 278 bp *pbpB* internal region was integrated into the chromosome through a single crossover. Transformants were selected for Erm^R with xylose added to the medium. For each of the 6 transformations, we did get a few transformant colonies (< 10 colonies/μg DNA) on plates. Because the 278 bp region came from the N domain of *pbpB*, for transformants that containing domain switch PBPs with PBP2b N domain (DPVB561, DPVB564, DPVB566), homologous recombination may occur either at the wild type *pbpB* locus or at the domain switch alleles. For the other strains (DPVB563, DPVB569, DPVB571), the insertion will only go into the wild type *pbpB* locus. For competent cell and plasmid controls, wild type PS832 strain was transformed with DPVB133 chromosomal DNA and pDPV362 plasmid, and the transformant numbers were 200 and 0 colonies/μg DNA, respectively.

After checking the chromosome of each experimental transformant by PCR reactions, we found that the wild type *pbpB* genes still existed in those strains. It is possible that the pDPV362 plasmid inserted into the chromosome at a position outside the *pbpB* gene through nonspecific recombination. This is a rare event but it can explain why there was only a small number of colonies, since this number for control experiments is 300-400 CFU. On the whole, it seems none of these domain switch PBPs

can complement wild type PBP2a/2b function.

Localization of PBP2a/PBP2b variants.

The six domain switch PBP2a/2b strains, grown to log-phase, were prepared to determine cellular localization by immunofluorescence microscopy. Cells were fixed, permeabilized, applied to slides, blotted, treated with anti-FLAG antibody and then incubated with biotinylated secondary antibody, streptavidin-linked Cy3 fluorophore and DAPI. For strains DPVB561, DPVB564, DPVB571, more than 90% of the cells (n>50) showed red bands or spots at midcell and cell poles with little or no Cy3 signal at other positions in the cell while the remaining 10% had no signals at midcell or poles or anywhere in the cell (Figure 9). These localization patterns are similar to that observed for PBP2b-FLAG in DPVB391 (Figure 8). For strains DPVB563, DPVB566, DPVB569, we observed Cy3 signals spread across the cylindrical wall for all the cells captured, and some of them (~60%) had obvious bands at the midcell (Figure 9). This is consistent with PBP2a-FLAG localizations (Figure 8).

We found that strains that contain the S domain of PBP2a have localization patterns resembling that of PBP2a, and those that contain the S domain of PBP2b have similar localization as PBP2b. These findings indicate that the S domains of PBB2a and PBP2b are the determinants for their cellular localization.

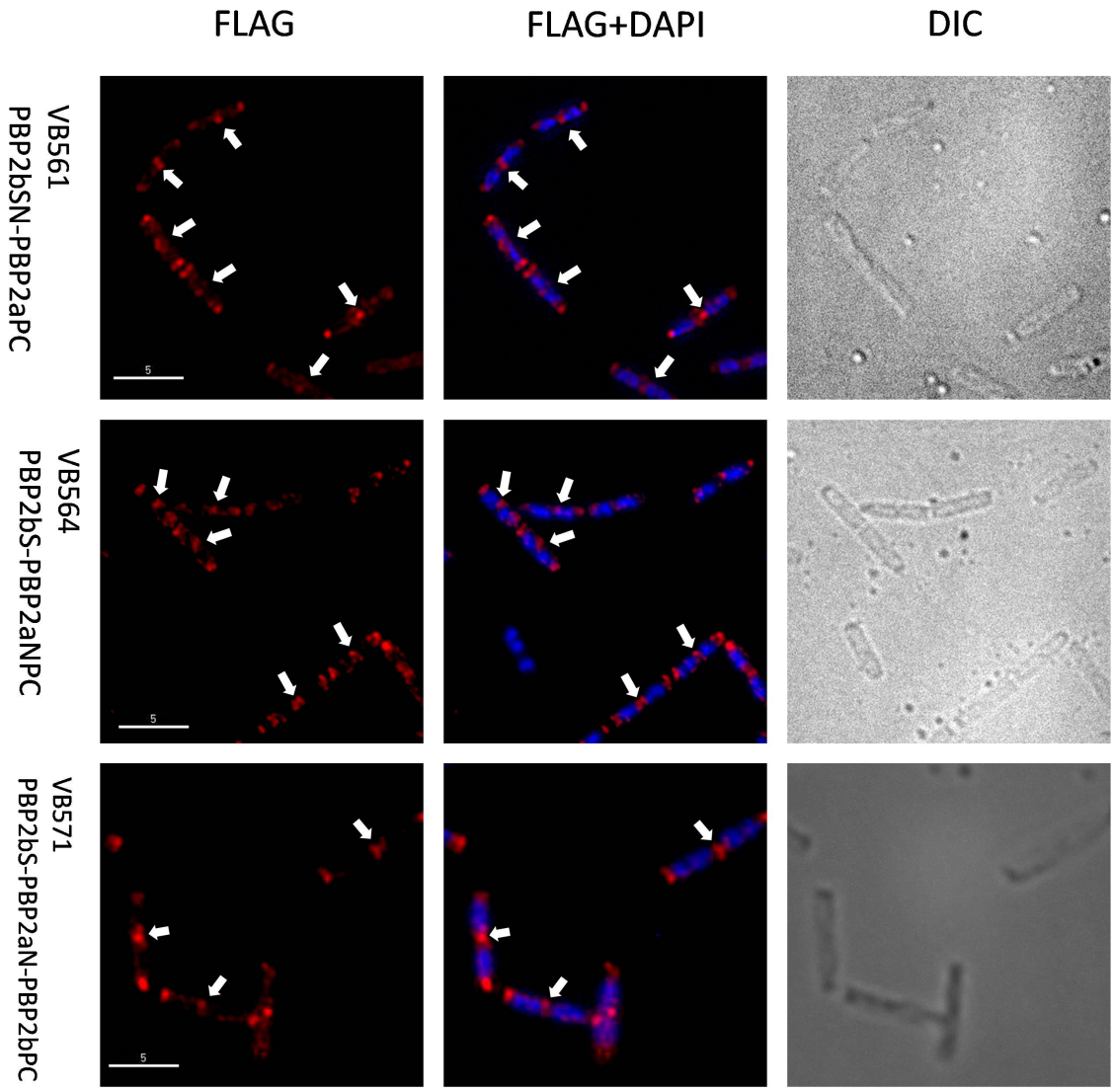

Figure 9. Localization of domain switch mutants. The figure shows a Cy3 staining of FLAG tagged PBPs (red), an overlay of DAPI staining of nucleoids (blue) and Cy3, and a differential interference contrast (DIC) image for comparison. Arrows point to PBP localizations at the midcell. The white bars represent 5 μm and all pictures are at the same magnification. Exposure time: 800 ms for DAPI and 500 ms for Cy3.

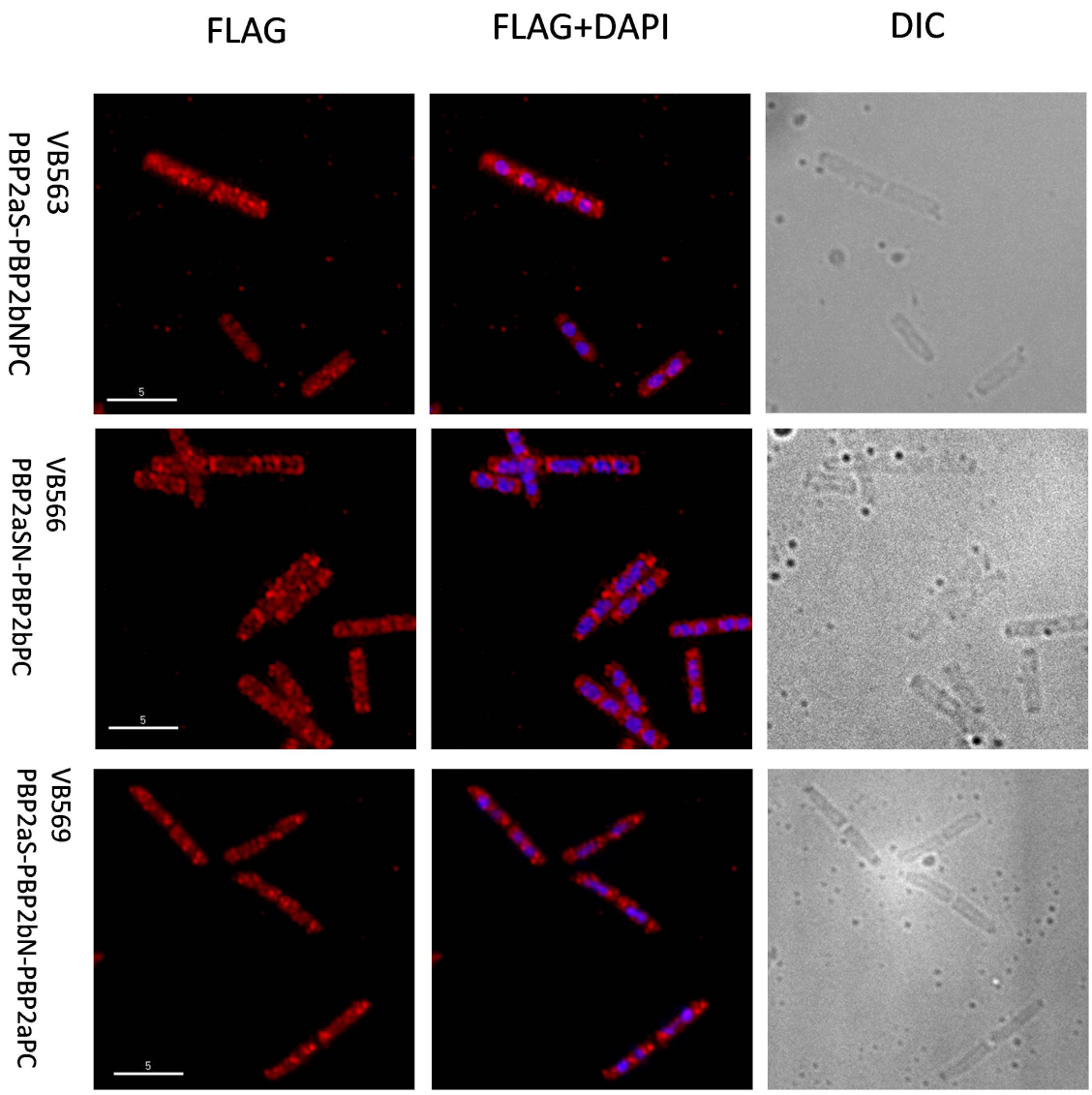

Figure 9 continued. Localization of domain switch mutants

Discussion

The structural determinant that directs PBP2a and PBP2b to their cellular membrane destinations was identified by constructing and analyzing a series of *B. subtilis* mutant strains in which the S domain, N domain, or S+N domain of PBP2a and PBP2b were switched between them. A FLAG tag was fused to the C-terminal of each protein. Expression of these proteins was examined by SDS-PAGE and Western blotting with anti-FLAG antibody. Functions of these proteins were studied through complementation assays. Finally, the localization patterns of these proteins were determined using immunofluorescence microscopy.

The FLAG epitope is composed of 8 amino acids (DYKDDDDK) and hydrophilic (pI=3.85), so it has a high probability of localizing at the protein surface when fused with a protein. FLAG tagged PBP2a and PBP2b can express full length proteins and were detected by the western blotting. Furthermore, C-terminal linked FLAG was found to have no negative effects on PBP2a and PBP2b functions since the native FLAG tagged proteins could fully complement functions of the non-tagged proteins. The FLAG epitope was also used to visualize PBP2a and PBP2b cellular localizations and we observed the expected localization patterns, which are consistent with previously observed results produced using GFP (53).

From the western blotting results (Figure 7), we observed that the protein bands of the 6 domain switch mutants have different abundances. PBP2aS-PBP2bNPC (lane 5) and PBP2aSN-PBP2bPC (lane 7) had bands as bright as the control native proteins (lane 2 and 3) while for other proteins (lane 3, 6, 8 and 9) there are very faint bands. The xylose promoter should drive equal expression of each of these proteins, so what causes the low level of those 4 proteins? The membrane preparation procedure was repeated several times, proteins were kept cold throughout the manipulation, and protease inhibitor

cocktail tablets and beta-mercaptoethanol were added to each buffer to prevent protein degradation. However, we got the same results every time. The weak signals are presumably due to the instability of these recombinant proteins. These domain-switch proteins were likely degraded during cell growth. From the immunofluorescence microscopy pictures we found the low abundance of these proteins didn't affect the detection of their localization.

For a complementation assay, in the *pbpH* strains expressing domain switch PBPs, the *pbpA* gene was deleted by transformed with the chromosomal DNA of *pbpA* strain (VB133). The resulting transformants were all nonviable. Similarly, the *pbpB* gene of the strains containing domain switch PBPs was knocked out by transforming pDPV362 plasmid with an internal 278bp *pbpB* region into it. Again, we got no viable transformants. These results indicate that both S and N domains are essential for the function of PBP2a and PBP2b. It was proposed that the transpeptidase module of *E. coli* Class B PBPs is regulated by the interaction of N domain with other proteins involved in the cell cycle (15,23). It is possible in the wild type cell, the S domain alone can direct the PBP2a/2b to their membrane positions, and then the N domain interacts with related proteins to assist the P domain to perform their transpeptidase activity. For recombinant proteins that have different S domains (PBP2bS-PBP2aNPC, PBP2bSN-PBP2aPC, PBP2aS-PBP2bNPC and PBP2aSN-PBP2bPC), they can not be transported to the desired place and can't perform their TP functions correctly. For those that have different N domains (PBP2aS-PBP2bN-PBP2aPC, PBP2bS-PBP2aN-PBP2bPC), the proteins may reach the correct location but either don't function correctly as a transpeptidase or don't interact properly with other components of the peptidoglycan synthesis machinery. A future experiment to measure the transpeptidase activity of these proteins can verify if the activity is functional. This can be done by determining the penicillin binding activities of these proteins since the transpeptidase catalyzes the same reactions when binding to

penicillin and PG substrates.

The PBP2a protein was known to have partial septum localization (53), so a portion of PBP2aS-PBP2bNPC protein should be correctly localized. However, this recombinant protein was still unable to complement wild type *pbpB'*s function. Possible explanations for this result are: 1. The "septum" may be a very complex site, and visual localization to the septum by both PBP2a and PBP2b could be in very different positions relative to the division machinery. 2. The cell's normal growth needs a greater amount of PBP2b. The PBP2aS-PBP2bNPC protein at the septum may not be enough to carry out normal PBP2b activity. 3. The S domain of PBP2b may also play some role in maintaining its TP activity, and changing to the PBP2a S domain causes PBP2b to work abnormally. To further examine the second possibility, we can change the S domain of PBP2b with S domain of PBP1, which has been known to localize specifically at the septum (53). If this strain is viable, the last hypothesis can be ruled out.

After learning that the S domain is the only requirement for PBP2a and PBP2b localization, we are still interested in identifying the specific regions in the S domains that target proteins to their destinations. In order to do this, we are going to construct a series of S domain truncated mutants of *pbpA* and *pbpB*, with FLAG fused to the 3' end. Then we will visualize the localizations and try to find out the minimal sequence requirements for their correct localizations.

References

1. **Anagnostopoulos, C. and J. Spizizen**. 1961. Requirements for transformation in *Bacillus subtilis*. J. Bacteriol. **81**:741-746.

2. **Beall, B. and J. Lutkenhaus**. 1989. Nucleotide sequence and insertional inactivation of a *Bacillus subtilis* gene that affects cell division, sporulation, and temperature sensitivity. J. Bacteriol. **171**:6821-6834.

3. **Beall, B. and J. Lutkenhaus**. 1992. Impaired cell division and sporulation of a *Bacillus subtilis* strain with the *ftsA* gene deleted. J. Bacteriol. **174**:2398-2403.

4. **Bhavsar, A. P., X. Zhao, and E. D. Brown**. 2001. Development and characterization of a xylose-dependent system for expression of cloned genes in *Bacillus subtilis*: conditional complementation of a teichoic acid mutant. Appl. Environ. Microbiol. **67**:403-410.

5. **Blumberg, P. M. and J. L. Strominger**. 1972. Five penicillin-binding components occur in *Bacillus subtilis* membranes. J. Biol. Chem. **247**:8107-8113.

6. **Blumberg, P. M. and J. L. Strominger**. 1972. Isolation by covalent affinity chromatography of the penicillin-binding components from membranes of *Bacillus subtilis*. Proc. Natl. Acad. Sci. U. S. A **69**:3751-3755.

7. **Boyle, D. S., M. M. Khattar, S. G. Addinall, J. Lutkenhaus, and W. D. Donachie**. 1997. *ftsW* is an essential cell-division gene in *Escherichia coli*. Mol. Microbiol. **24**:1263-1273.

8. **Contreras-Martel, C., V. Job, A. M. Di Guilmi, T. Vernet, O. Dideberg, and A. Dessen**. 2006. Crystal structure of penicillin-binding protein 1a (PBP1a) reveals a mutational hotspot implicated in beta-lactam resistance in *Streptococcus pneumoniae*. J. Mol. Biol. **355**:684-696.

9. **Daniel, R. A., S. Drake, C. E. Buchanan, R. Scholle, and J. Errington**. 1994. The *Bacillus subtilis spoVD* gene encodes a mother-cell-specific penicillin-binding protein required for spore morphogenesis. J. Mol. Biol. **235**:209-220.

10. **Daniel, R. A. and J. Errington**. 2000. Intrinsic instability of the essential cell

division protein FtsL of *Bacillus subtilis* and a role for DivIB protein in FtsL turnover. Mol. Microbiol. **36**:278-289.

11. **David White**. 2000. Cell wall and capsule biosynthesis, p. 295-313. *In* The physiology and biochemistry of prokaryotes. Oxford University Press, Inc.

12. **Den, B. T., N. Buddelmeijer, M. E. Aarsman, C. M. Hameete, and N. Nanninga**. 1999. Timing of FtsZ assembly in *Escherichia coli*. J. Bacteriol. **181**:5167-5175.

13. **Dessen, A., N. Mouz, E. Gordon, J. Hopkins, and O. Dideberg**. 2001. Crystal structure of PBP2x from a highly penicillin-resistant *Streptococcus pneumoniae* clinical isolate: a mosaic framework containing 83 mutations. J. Biol. Chem. **276**:45106-45112.

14. **Dijkstra, A. J.** 1997. The lytic transglycosylase family of *Escherichia coli* : in vitro activity versus in vivo function.(phD dissertation, University of Groningen, 1997). p. 1-35.

15. **Eberhardt, C., L. Kuerschner, and D. S. Weiss**. 2003. Probing the catalytic activity of a cell division-specific transpeptidase in vivo with beta-lactams. J. Bacteriol. **185**:3726-3734.

16. **Errington, J., R. A. Daniel, and D. J. Scheffers**. 2003. Cytokinesis in bacteria. Microbiol. Mol. Biol. Rev. **67**:52-65.

17. **Feucht, A., I. Lucet, M. D. Yudkin, and J. Errington**. 2001. Cytological and biochemical characterization of the FtsA cell division protein of *Bacillus subtilis*. Molecular Microbiology **40**:115-125.

18. **Foster, S. J. a. D. L. P.** 2001. Structure and synthesis of cell wall, spore cortex, teichoic acids, S-layers, and capsules, p. 21-41. *In Bacillus subtilis* and Its Close Relatives: From Genes to Cells. American Society for Microbiology, Washington, D.C.

19. **Ghuysen, J. M.** 1991. Serine beta-lactamases and penicillin-binding proteins. Annu. Rev. Microbiol. **45**:37-67.

20. **Goffin, C. and J. M. Ghuysen**. 2002. Biochemistry and comparative genomics of SxxK superfamily acyltransferases offer a clue to the mycobacterial paradox: presence of penicillin-susceptible target proteins versus lack of efficiency of penicillin as therapeutic agent. Microbiol. Mol. Biol. Rev. **66**:702-38, table.

21. **Goffin, C. and J. M. Ghuysen**. 1998. Multimodular penicillin-binding proteins:

an enigmatic family of orthologs and paralogs. Microbiol. Mol. Biol. Rev. **62**:1079-1093.

22. **Henriques, A. O., P. Glaser, P. J. Piggot, and C. P. Moran, Jr.** 1998. Control of cell shape and elongation by the *rodA* gene in *Bacillus subtilis*. Mol. Microbiol. **28**:235-247.

23. **Holtje, J. V.** 1998. Growth of the stress-bearing and shape-maintaining murein sacculus of *Escherichia coli*. Microbiol. Mol. Biol. Rev. **62**:181-203.

24. **Ikeda, M., T. Sato, M. Wachi, H. K. Jung, F. Ishino, Y. Kobayashi, and M. Matsuhashi**. 1989. Structural similarity among Escherichia coli FtsW and RodA proteins and *Bacillus subtilis* SpoVE protein, which function in cell division, cell elongation, and spore formation, respectively. J. Bacteriol. **171**:6375-6378.

25. **Jones, L. J., R. Carballido-Lopez, and J. Errington**. 2001. Control of cell shape in bacteria: helical, actin-like filaments in *Bacillus subtilis*. Cell **104**:913-922.

26. **Karczmarek, A., R. Martinez-Arteaga, S. Alexeeva, F. G. Hansen, M. Vicente, N. Nanninga, and B. T. Den**. 2007. DNA and origin region segregation are not affected by the transition from rod to sphere after inhibition of *Escherichia coli* MreB by A22. Mol. Microbiol. **65**:51-63.

27. **Karimova, G., N. Dautin, and D. Ladant**. 2005. Interaction network among *Escherichia coli* membrane proteins involved in cell division as revealed by bacterial two-hybrid analysis. J. Bacteriol. **187**:2233-2243.

28. **Katis, V. L., R. G. Wake, and E. J. Harry**. 2000. Septal localization of the membrane-bound division proteins of *Bacillus subtilis* DivIB and DivIC is codependent only at high temperatures and requires FtsZ. J. Bacteriol. **182**:3607-3611.

29. **Kelly, J. A., A. P. Kuzin, P. Charlier, and E. Fonze**. 1998. X-ray studies of enzymes that interact with penicillins. Cell Mol. Life Sci. **54**:353-358.

30. **Khattar, M. M., K. J. Begg, and W. D. Donachie**. 1994. Identification of *FtsW* and characterization of a new *ftsW* division mutant of *Escherichia coli*. J. Bacteriol. **176**:7140-7147.

31. **Krauss, J., L. M. van der, T. Grebe, and R. Hakenbeck**. 1996. Penicillin-binding proteins 2x and 2b as primary PBP targets in *Streptococcus*

pneumoniae. Microb. Drug Resist. **2**:183-186.

32. **Kruse, T., J. Bork-Jensen, and K. Gerdes**. 2005. The morphogenetic MreBCD proteins of *Escherichia coli* form an essential membrane-bound complex. Mol. Microbiol. **55**:78-89.

33. **Kruse, T., J. Bork-Jensen, and K. Gerdes**. 2005. The morphogenetic MreBCD proteins of *Escherichia coli* form an essential membrane-bound complex. Mol. Microbiol. **55**:78-89.

34. **Kruse, T., J. oller-Jensen, A. obner-Olesen, and K. Gerdes**. 2003. Dysfunctional MreB inhibits chromosome segregation in *Escherichia coli*. EMBO J. **22**:5283-5292.

35. **Laible, G. and R. Hakenbeck**. 1991. Five independent combinations of mutations can result in low-affinity penicillin-binding protein 2x of *Streptococcus pneumoniae*. J. Bacteriol. **173**:6986-6990.

36. **Lee, S. and C. W. Price**. 1993. The *minCD* locus of *Bacillus subtilis* lacks the *minE* determinant that provides topological specificity to cell division. Mol. Microbiol. **7**:601-610.

37. **Leighton, T. J. and R. H. Doi**. 1971. The stability of messenger ribonucleic acid during sporulation in *Bacillus subtilis*. J. Biol. Chem. **246**:3189-3195.

38. **Levin, P. A. and R. Losick**. 1994. Characterization of a cell division gene from *Bacillus subtilis* that is required for vegetative and sporulation septum formation. J. Bacteriol. **176**:1451-1459.

39. **Lowry, O. H., N. J. Rosebrough, A. L. Farr, and R. J. Randall**. 1951. Protein measurement with the Folin phenol reagent. J. Biol. Chem. **193**:265-275.

40. **Marston, A. L., H. B. Thomaides, D. H. Edwards, M. E. Sharpe, and J. Errington**. 1998. Polar localization of the MinD protein of *Bacillus subtilis* and its role in selection of the mid-cell division site. Genes Dev. **12**:3419-3430.

41. **Matsuhashi, M., M. Wachi, and F. Ishino**. 1990. Machinery for cell growth and division: penicillin-binding proteins and other proteins. Res. Microbiol. **141**:89-103.

42. **Matsuzawa, H., S. Asoh, K. Kunai, K. Muraiso, A. Takasuga, and T. Ohta**. 1989. Nucleotide sequence of the *rodA* gene, responsible for the rod shape of *Escherichia coli*: *rodA* and the *pbpA* gene, encoding penicillin-binding protein 2, constitute the *rodA* operon. J. Bacteriol. **171**:558-560.

43. **Mercer, K. L. and D. S. Weiss**. 2002. The *Escherichia coli* cell division protein FtsW is required to recruit its cognate transpeptidase, FtsI (PBP3), to the division site. J. Bacteriol. **184**:904-912.

44. **Murray, T., D. L. Popham, and P. Setlow**. 1997. Identification and characterization of *pbpA* encoding *Bacillus subtilis* penicillin-binding protein 2A. J. Bacteriol. **179**:3021-3029.

45. **Pares, S., N. Mouz, Y. Petillot, R. Hakenbeck, and O. Dideberg**. 1996. X-ray structure of *Streptococcus pneumoniae* PBP2x, a primary penicillin target enzyme. Nat. Struct. Biol. **3**:284-289.

46. **Pedersen, L. B., E. R. Angert, and P. Setlow**. 1999. Septal localization of penicillin-binding protein 1 in *Bacillus subtilis*. J. Bacteriol. **181**:3201-3211.

47. **Piette, A., C. Fraipont, B. T. Den, M. E. Aarsman, S. Pastoret, and M. Nguyen-Disteche**. 2004. Structural determinants required to target penicillin-binding protein 3 to the septum of *Escherichia coli*. J. Bacteriol. **186**:6110-6117.

48. **Pla, J., M. Sanchez, P. Palacios, M. Vicente, and M. Aldea**. 1991. Preferential cytoplasmic location of FtsZ, a protein essential for *Escherichia coli* septation. Mol. Microbiol. **5**:1681-1686.

49. **Popham, D. L. and P. Setlow**. 1996. Phenotypes of *Bacillus subtilis* mutants lacking multiple class A high-molecular-weight penicillin-binding proteins. J. Bacteriol. **178**:2079-2085.

50. **Popham, D. L. and P. Setlow**. 1995. Cloning, nucleotide sequence, and mutagenesis of the *Bacillus subtilis ponA* operon, which codes for penicillin-binding protein (PBP) 1 and a PBP-related factor. J. Bacteriol. **177**:326-335.

51. **Sauvage, E., F. Kerff, M. Terrak, J. A. Ayala, and P. Charlier**. 2008. The penicillin-binding proteins: structure and role in peptidoglycan biosynthesis. FEMS Microbiol. Rev. **32**:234-258.

52. **Scheffers, D. J.** 2005. Dynamic localization of penicillin-binding proteins during spore development in *Bacillus subtilis*. Microbiology **151**:999-1012.

53. **Scheffers, D. J., L. J. F. Jones, and J. Errington**. 2004. Several distinct localization patterns for penicillin-binding proteins in *Bacillus subtilis*. Molecular Microbiology **51**:749-764.

54. **Shih, Y. L., T. Le, and L. Rothfield**. 2003. Division site selection in *Escherichia coli* involves dynamic redistribution of Min proteins within coiled structures that extend between the two cell poles. Proc. Natl. Acad. Sci. U. S. A **100**:7865-7870.

55. **Sievers, J. and J. Errington**. 2000. The *Bacillus subtilis* cell division protein FtsL localizes to sites of septation and interacts with DivIC. Mol. Microbiol. **36**:846-855.

56. **Spratt, B. G.** 1975. Distinct penicillin binding proteins involved in the division, elongation, and shape of Escherichia coli K12. Proc. Natl. Acad. Sci. U. S. A **72**:2999-3003.

57. **Spratt, B. G.** 1975. Distinct penicillin binding proteins involved in the division, elongation, and shape of *Escherichia coli* K12. Proc. Natl. Acad. Sci. U. S. A **72**:2999-3003.

58. **Steinmetz, M. and R. Richter**. 1994. Plasmids designed to alter the antibiotic resistance expressed by insertion mutations in *Bacillus subtilis*, through in vivo recombination. Gene **142**:79-83.

59. **Tamaki, S., H. Matsuzawa, and M. Matsuhashi**. 1980. Cluster of *mrdA* and *mrdB* genes responsible for the rod shape and mecillinam sensitivity of *Escherichia coli*. J. Bacteriol. **141**:52-57.

60. **van den, E. F., M. Leaver, F. Bendezu, J. Errington, B. P. de, and J. Lowe**. 2006. Dimeric structure of the cell shape protein MreC and its functional implications. Mol. Microbiol. **62**:1631-1642.

61. **van, H. J.** 2001. Recent advances in the formation of the bacterial peptidoglycan monomer unit. Nat. Prod. Rep. **18**:503-519.

62. **Wachi, M., M. Doi, Y. Okada, and M. Matsuhashi**. 1989. New *mre* genes *mreC* and *mreD*, responsible for formation of the rod shape of *Escherichia coli* cells. J. Bacteriol. **171**:6511-6516.

63. **Wang, X., J. Huang, A. Mukherjee, C. Cao, and J. Lutkenhaus**. 1997. Analysis of the interaction of FtsZ with itself, GTP, and FtsA. J. Bacteriol. **179**:5551-5559.

64. **Wei, Y., T. Havasy, D. C. McPherson, and D. L. Popham**. 2003. Rod shape determination by the *Bacillus subtilis* class B penicillin-binding proteins encoded by *pbpA* and *pbpH*. J. Bacteriol. **185**:4717-4726.

65. **Wei, Y., D. C. McPherson, and D. L. Popham**. 2004. A mother cell-specific class B penicillin-binding protein, PBP4b, in **Bacillus subtilis**. J. Bacteriol. **186**:258-261.

66. **Wissel, M. C. and D. S. Weiss**. 2004. Genetic analysis of the cell division protein FtsI (PBP3): amino acid substitutions that impair septal localization of FtsI and recruitment of FtsN. J. Bacteriol. **186**:490-502.

67. **Wu, L. J., A. H. Franks, and R. G. Wake**. 1995. Replication through the terminus region of the *Bacillus subtilis* chromosome is not essential for the formation of a division septum that partitions the DNA. J. Bacteriol. **177**:5711-5715.

68. **Yanouri, A., R. A. Daniel, J. Errington, and C. E. Buchanan**. 1993. Cloning and sequencing of the cell division gene *pbpB*, which encodes penicillin-binding protein 2B in *Bacillus subtilis*. J. Bacteriol. **175**:7604-7616.